

Characterization of defects in composite materials by the intrusive stochastic method using the Gaussian type random variable

Abstract. In this work, we propose an approach for the characterization of a composite plate and the evaluation of defects. This approach, called the intrusive stochastic finite element method (ISFEM), consists in considering electrical conductivity as a random variable. The inspection will be done by the non-destructive testing process by eddy currents. The results obtained for two applications are compared with experimental data and those of the Benchmark JSAEM#Problem1.

Streszczenie. W tej pracy proponujemy podejście do charakteryzacji płyty kompozytowej i oceny wad. Podejście to, zwane inwazyjną metodą stochastycznych elementów skończonych (ISFEM), polega na uznaniu przewodnictwa elektrycznego za zmienną losową. Inspekcja zostanie przeprowadzona metodą badań nieniszczących prądami wirowymi. Wyniki uzyskane dla dwóch aplikacji są porównywane z danymi eksperymentalnymi i wynikami testu porównawczego JSAEM#Problem1. (**Charakterystyka defektów w materiałach kompozytowych metodą stochastyczną inwazyjną z wykorzystaniem zmiennej losowej typu Gaussa**)

Keywords: Composite materials - Intrusive stochastic finite element - Random variable - Impedance variation

Słowa kluczowe: Materiały kompozytowe - Inwazyjny stochastyczny element skończony - Zmienna losowa - Zmiana impedancji

Introduction

We can attribute to composites, according to their different constituents and their implementation processes, remarkable physical and mechanical properties (rigidity, high temperature resistance, corrosion resistance, etc.) and lightness. These types of materials are found in many fields such as aeronautics especially, shipbuilding, railways, civil engineering. The mechanical and electrical characteristics of composites can only be estimated after manufacture, unlike conventional materials such as aluminum, carbon, etc.

Different techniques aim to characterize these materials (measurement of their thickness or detection of surface or internal defects) [1 2].

Among these different techniques, non-destructive testing by eddy current (NDT-EC), remains a powerful tool for inspecting the quality and reliability of a composite material. Its real-time operation has become necessary in industrial environments and other applications [3].

CFRP-type composite materials, being electrically conductive, can be inspected by eddy current testing summarizes all the promising application aspects of Eddy's current CFRP inspection methods, including fiber orientation measurements and testing for crack delamination and fiber breakage [4 5]. Only the majority of methods proposed in the NDT-EC for condition inspection of composites require inverse problem solving to recover impedance, and for reliability assessment require a probabilistic or other method, which generates a very significant simulation time, without forgetting the experimental tests which remain of course reliable, require equipment that is sometimes inaccessible or even expensive, the times for carrying out experiments are significant.

In order to complete this very rich database, we propose as part of our study, a numerical model based on the intrusive stochastic finite element method (ISFEM), executed under a Matlab environment.

This proposed approach, associated with NDT-CE, allows the processing and post-processing of the defect evaluation problem in a single step,

Despite the tensorial nature of the electrical conductivity of CFRP, it has been shown

that longitudinal conductivity predominates over transverse conductivity [6 7 8],

The fibers in a unidirectional CFRP have an inclination between 0.2° and 1° around their axis [GOMES09]; which allows contact between fibers and consequently the creation of current loops.

All these observations make it possible to opt for a 2D approach for the modeling of CND-EC [9 10].

The longitudinal electrical conductivity σ_L will be considered, the random variable, of Gaussian type and the orientation will be along the x axis. A distribution of the random variable in Hermite polynomials is made based on the degree of polynomial chaos p . The simulation of the NDT-EC problem is obtained on the basis of resolution of the magnetodynamic equation in terms of potential magnetic vector A , in axisymmetric hypothesis 2D.

The latter will generate a number of solutions equal to p . The solutions obtained in terms of vector potential A are random. The calculation of the impedance Z is derived using a method based on the solutions A . An evaluation of the impedance in the presence and in the absence of the fault is carried out. The variation of Z is obtained when moving the absolute sensor along a composite plate without defect, and along the defect zone [11].

This process is carried out on two distinct applications which allowed us to validate our stochastic model (ISFEM).

The first application is carried out on a piece of Inconel 600 according to the data provided by the experimental.

This experimental part is carried out at the Research Center for Real Time NDT Chosun University Gwangju, South Korea. The NORTEK 500 series eddy current fault detection device is connected to a laptop computer containing LabVIEW and is used to characterize and evaluate Inconel 600 faults.

A second application is carried out with reference to Benchmark JSAEM#Problème1 [12], the results obtained during the simulations are confronted with it.

The reliability study is represented by the evaluation of the reliability index β of the system. The Synthesis flowchart under Matlab is given at figure 13.

Deterministic magnetodynamic model

To simulate an electromagnetic problem in NDT-CF, it is necessary to set up a mathematical model. The latter is obtained from Maxwell's equations, constitutive laws and boundary conditions. It is necessary to define the fields of definition of the electric and magnetic variables and the differential operators.

In the literature several formulations are developed to represent the magnetodynamic model describing the problems where currents are induced by variable magnetic fields [13 14].

The electromagnetic equation is obtained with the consideration of assumptions that the displacement currents are negligible and the volume charge density is assumed to be zero [15 16]. There by the relationship between the magnetic field and current which flows in the conducting media is given by the Maxwell equation below

In the case of our study, we exploit the magnetodynamic formulation in vector potential

\vec{A} , in harmonic hypothesis, given as follows [11]:

$$\begin{aligned} (1) \quad \vec{\nabla} \wedge \vec{H} &= \vec{J}_c \\ (2) \quad \vec{J}_c &= \vec{J}_s - \sigma \frac{\partial \vec{A}}{\partial t} \\ (3) \quad \vec{H} &= \nu \vec{B} \\ (4) \quad \vec{B} &= \vec{\nabla} \wedge \vec{A} \\ (5) \quad \vec{\nabla} \wedge (\nu \vec{\nabla} \wedge \vec{A}) + j\sigma\omega \vec{A} &= \vec{J}_s \end{aligned}$$

\vec{B} and \vec{H} are the magnetic flux density [T] and the magnetic field [A/m] respectively. \vec{J}_c is the total current density [A/m²], \vec{J}_s is the source current density [A/m²], ν : Magnetic reluctivity [H / m]⁻¹, σ : Electric conductivity [Ω m]⁻¹ and ω is the angular frequency.

Formulation of the electrical conductivity tensor

The equivalent conductivity σ of CFRP composites is a tensor. For monolayers and laminates that have the same layer orientations, modeling CFRP composites represented by conductive plates of equivalent anisotropic conductivities is effective [12]. Considering that the fibers are oriented at some arbitrary angle θ with respect to the x-axis, the generalized conductivity matrix of the composite CFRP can be deduced as follows[6 10] :

$$(6) \quad [\sigma] = \begin{bmatrix} \sigma_L \cos^2 \theta + \sigma_T \sin^2 \theta & \frac{\sigma_L - \sigma_T}{2} \sin^2 \theta & 0 \\ \frac{\sigma_L - \sigma_T}{2} \sin^2 \theta & \sigma_L \sin^2 \theta + \sigma_T \cos^2 \theta & 0 \\ 0 & 0 & \sigma_{cp} \end{bmatrix}$$

In the case of our study the fibers are oriented along the x axis, hence $\theta = 0$.

We find the following conductivity tensor:

$$(7) \quad [\sigma] = \begin{bmatrix} \sigma_L & 0 & 0 \\ 0 & \sigma_T & 0 \\ 0 & 0 & \sigma_{cp} \end{bmatrix}$$

Where [9]

$$(8) \quad \sigma_{cp} \ll \sigma_T \ll \sigma_L$$

σ_L , σ_T , σ_{cp} are respectively longitudinal, transverse and interply conductivity.

Formulation of the stochastic algebraic system

The magnetic vector potential A , is the unknown in our algebraic system, its expression as a random variable in the basis of Hermit's polynomials is given as follows:

$$(9) \quad A = \sum_{j=0}^{n_A} A_j \Psi_j(\xi_1, \dots, \xi_M)$$

Random Electrical Conductivity

The electrical conductivity σ_L , input variable, being the hazard on the physical property, this one is distributed over the polynomial chaos as a random variable of the Gaussian type, characterized by an average value and a standard deviation. Its expression in the base of Hermit's polynomials is given below:

$$(10) \quad \sigma_L = \sum_{i=1}^{p-1} \sigma_{L_i} H_i(\xi_1, \dots, \xi_M)$$

After development, by considering a random variable of the Gaussian type characterized by an average value σ_{L0} and a standard deviation E_c (represents a percentage of σ_{L0}), we obtain the following matrix σ_{Ls} :

$$(11) \quad \sigma_{Ls} = \begin{bmatrix} \sigma_{L0} & E_c & 0 \\ E_c & \sigma_{L0} & 2 * E_c \\ 0 & 2 * E_c & 2 * \sigma_{L0} \end{bmatrix}$$

The non-destructive testing by eddy current applied in our study is built taking into account the fact that the current density of the source and the electrical conductivity according to the orientation of the fibers σ_L of the composite material is given.

The minimization when using Galerkin method means requiring the orthogonality of the residue with the base of projection functions $\{\psi_j, j = 0 \dots p\}$. By taking as test

function α_i the chaos polynomial ψ_j . This leads to [11].

$$(12) \quad \sum_{j=0}^{p-1} M_0 A_j E[\psi_j \psi_k] + \sum_{i=0}^{p-1} \sum_{j=0}^{p-1} N_i A_j E[\psi_i \psi_j \psi_k]$$

$$k = 0, \dots, p-1$$

The final form of the intrusive stochastic finite element method and harmonic linear system is:

$$(13) \quad F_k^{st} = \sum_{j=0}^{p-1} (M_{jk}^{st} + j\omega N_{jk}^{st}) A_j$$

$$(14) \quad M_{jk}^{st} = x_{0jk} M_0$$

$$(15) \quad N_{jk}^{st} = \sum_{i=0}^{p-1} x_{ijk} N_i^{st}$$

$$(16) \quad x_{ijk} = \begin{cases} \frac{i!j!k!}{\left(\frac{i+j-k}{2}\right)!\left(\frac{j+k-i}{2}\right)!\left(\frac{k+i-j}{2}\right)!} & \text{if } \begin{cases} (i+j+k) \text{ even} \\ k \in [i-j, i+j] \end{cases} \\ 0 & \text{otherwise} \end{cases}$$

M^{st} , N^{st} , F^{st} are the random linear matrixes and source vector respectively related to solving problem. The stochastic system obtained from (16) is:

$$(17) \quad \begin{bmatrix} E_{00}^{st} & E_{10}^{st} & E_{20}^{st} \\ E_{01}^{st} & E_{11}^{st} & E_{21}^{st} \\ E_{02}^{st} & E_{12}^{st} & E_{22}^{st} \end{bmatrix} \begin{bmatrix} A_0 \\ A_1 \\ A_2 \end{bmatrix} = \begin{bmatrix} F_0 \\ F_1 \\ F_2 \end{bmatrix}$$

The expression of the resulting matrix E is obtained by equations (14), (15) as follows:

$$(18) E_{jk}^{st} = M_{jk}^{st} + j\omega N_{jk}^{st}$$

The solutions obtained after solving the stochastic complex algebraic system are A_0 , A_1 , A_2 and the

components of the source vector are F_0, F_1, F_2

Post treatment

The calculation of the impedance is obtained from the electromagnetic energy of the coil, hence the exploitation of the solutions of the vector potential A . The number of solution for A and the impedance Z is equal to p , which represents the degree of polynomial chaos.

The formulations of the real and imaginary part of the impedance Z , during characterization and in the suspected fault zone are given as follows [11]:

$$(19) \text{Re}(Z) = -\frac{N^2}{J \cdot S^2} \omega \cdot \iint_S 2 \cdot \pi \cdot r \cdot \text{Im}(A) \cdot ds$$

$$(20) \text{Im}(Z) = \frac{N^2}{J \cdot S^2} \omega \cdot \iint_S 2 \cdot \pi \cdot r \cdot \text{Re}(A) \cdot ds$$

with N : coils number, S : surface of inductor coil, r : inductor radius, $\text{Re}(A)$ and $\text{Im}(A)$ are real and imaginary parts of magnetic vector potential respectively.

The variation of the impedance Z in the crack is calculated as follows:

$$(21) \Delta Z = \|Z_p - Z_0\|$$

Where Z_p and Z_0 represent respectively the impedance of the plate with fault and without fault.

The reliability index β

The intrusive stochastic finite element method allows us to directly assess the reliability of our studied system, by determining the limit state function G_{ISFEM} and the reliability index β [17 18].

We just have to exploit the three impedances resulting from the stochastic calculation and the reference impedance Z_0 without the presence of a fault.

The expressions are given as follows:

$$(22) G_{ISFEM} = Z_0 - \sum_{p=0}^{p=2} Z_p ; \sum_{p=0}^{p=2} Z_p = Z_{p=0} + Z_{p=1} + Z_{p=2}$$

Where $Z_{p=0}, Z_{p=1}, Z_{p=2}$ are the three impedances derived from the three solutions of the magnetic vector potential A

$$(23) \beta = \text{Min} \sqrt{G_{ISFEM}}$$

Description of the applications

Application 1

To first validate our stochastic model; we carried out simulations with reference to the experimental carried out at the Research Center for Real Time NDT Chosun University Gwangju, South Korea.

This experiment relates to the characterization of the base alloy Nickel (Inconel600), the experiment makes it possible to recover at the same time the amplitude as well as the angle with Nortek 500. A frequency probe of 100kHz-500kHz with Lab VIEW. These two quantities were exploited in order to estimate the dimensions of the crack (the size and the depth).

The Inconel600 plate contains an artificial defect of rectangular shape having a constant length and width. The scan is carried out for depths of 100% air, 50% and 10%. In the simulation, the depths correspond to the standard deviation of the random variable σ_L . The frequency is 150 KHz;

The geometry of the device is reported in figure 1,

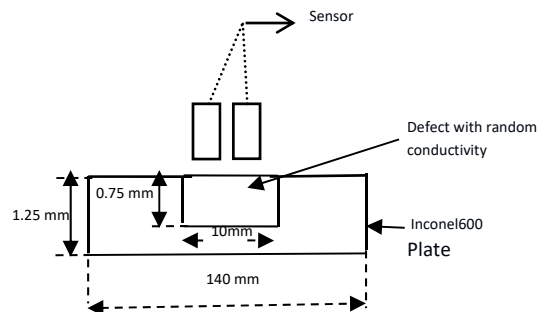


Fig.1. Geometry description

The geometric and physical data are given in table1.

Table1: Parameters of the application

Inducteur	Plate	Defect
Inner diameter 10mm	Thickness 2 mm	Length 10 mm
Outer diameter 12mm	Conductivity $\sigma_{L0} = 1 \times 10^6$ S/m	Width 0.75 mm Depth 1mm
Height 0.8mm	Relative permeability 1	$E_{C1}=0.1$ $E_{C2}=0.5$ $E_{C3}=0.9$
Number of turns 200	Lift-off 1 mm	Frequency 150Khz

Results and interpretation

The results obtained are shown by Fig.2, Fig.3, Fig.4, Fig.5 and Fig.6.

Figure.2 shows the mesh of the domain of study of the defect with rectangular geometry. This mesh is used for the resolution of the axisymmetric 2D electromagnetic system.

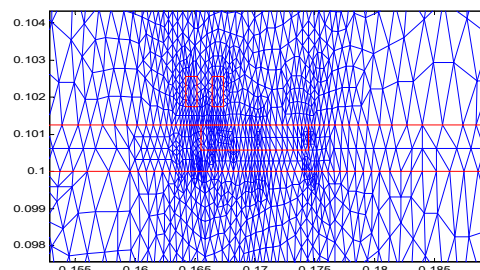


Fig.2. Mesh of the studied domain for rectangular geometry

Figure 3 represents the distribution of the vector potential A ($p=0$), one of the three stochastic solutions.

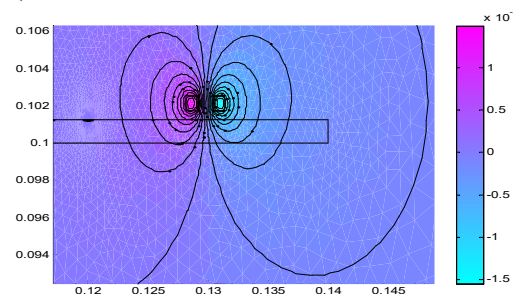


Fig.3. Distribution of vector potential A ($p=0$)

Figure 4 shows us the three stochastic solutions for $p=0,1,2$, of the variation of the impedance Z , they are practically the same, for this reason, the following results are given for a single solution for $p=0$.

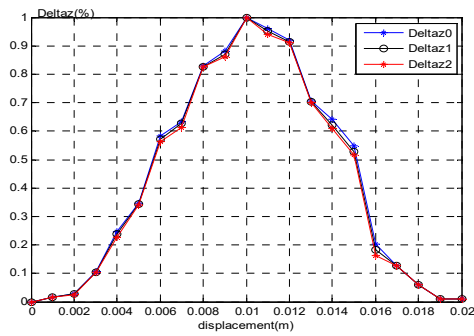


Fig.4. The three stochastic solutions of the variation of the impedance Z

Figure 5 shows the comparison of the variation of the impedance in reduced value resulting from the ISFEM calculation and the experimental one, when the penetration is 100%, this results in $\sigma_{L0}=0, E_C=0$.

We find a good agreement between the experiment and the stochastic calculation. This amounts to the 2D approximation, since the experiment is carried out in 3D.

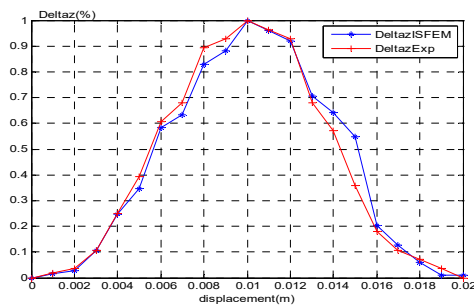


Fig.5. Deltaz resulting from the ISFEM calculation and the experimental

Figure 6 shows us the comparison of impedance variations for different standard deviations E_c . Figure 5 shows us the comparison of the variations of impedances for different standard deviations E_c . We note the influence of the standard deviation on the variation of the impedance. For each standard deviation, the stochastic matrix of the electrical conductivity is deduced, hence a penetration rate in the fault zone.

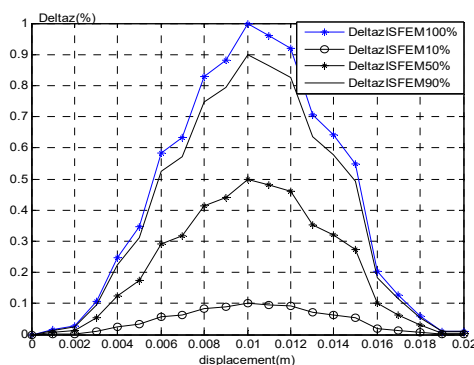


Fig.6. comparison of the variations of impedances for different standard deviations E_c

Application2

In eq. (6), σ_L is the longitudinal conductivity. Carbon fibers give rise to σ_L along the orientation of the fiber. Following contact between adjacent fibers and plies, the conductivities σ_T and σ_{cp} respectively transverse and between plies are induced [5 9]. The values of the electrical conductivities measured vary between 5×10^3 and 5×10^4

S/m in the fiber direction, and between 10 and 10^2 S/m in the transverse direction.

The conductivity of cross folds σ_{cp} is of lower value, it is usually half the value of σ_T , which is attributed to the existence of resin-rich interlaminar regions in the thickness direction [6 9].

The ISFM model consists of an air core coil on top of a CFRP plate. Table 2 summarizes some test conditions. Figures 7 and 8, respectively show the coil and the plate with crack and without crack.

The sample dimensions of the probe and the CFRP plate are considered based on the JSAEM#Problem1 benchmark [12]. The predictions of the coil impedance variation are compared with those obtained by the experimental measurements of the benchmark, which are given in Table 3.

Table2: Configurations of coil and Plate

Coil	Plate	Defect
Inner diameter: 1.2 mm	Height 40mm	Length 10 mm Width 0.2mm Depth 1.25mm
Outer diameter: 3.2 mm	Width 40mm	
Height 0.8 mm	Thickness 1.25 mm	
Width 1.0 mm	Relative permeability 1	
Current 1/140 A	Lift-off 0.5 mm	
Number of turns: 140		

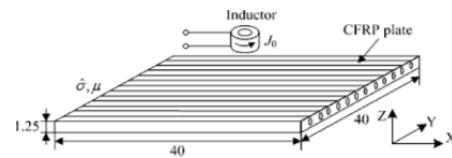


Fig.7. NDT-EC device Coil and CFRP plate without crack

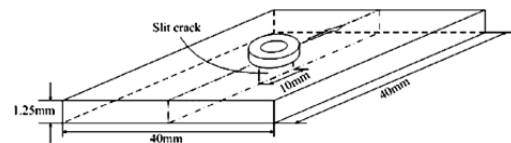


Fig.8. NDT-EC device Coil and CFRP plate with crack

Determination of the orientation of carbon fibers

In the case of CFRP laminates, the conductivity tensor given in Eq. (6) can be used to indicate The orientation angle of the carbon fibers.

Either, when all CFRP plies are stacked along the x axis, the angle $\theta = 0^\circ$ and along the y axis $\theta = 90^\circ$. The conductivity tensor in Equation. (7) becomes as follows:

$$(22) \quad [\sigma_{CFRP}] = \begin{bmatrix} \sigma_L = 5 \times 10^4 & 0 & 0 \\ 0 & \sigma_T = 100 & 0 \\ 0 & 0 & \sigma_{cp} = 50 \end{bmatrix}$$

Table3. The predictions of the coil impedance variation

Frequency	Simulation ISFEM	$Z_{ISFEM} = -0.89 + 0.76i$ [Ω]
150 KHZ	Experiment	$Z_{Exp} = -0.99 + 0.79i$ [Ω]

The two impedances are formulated in exponential form below:

$$Z_{ISFEM} = \|Z_{ISFEM}\| e^{i\varphi}$$

$$Z_{Exp} = \|Z_{Exp}\|e^{i\alpha}$$

$\|Z_{ISFEM}\|$ and $\|Z_{Exp}\|$: The modulus of impedance

φ, α : Argument of The impedance

The evolution of these two impedances according to their respective arguments given in figure 9, shows an excellent concordance which reinforces the stochastic model ISFEM.

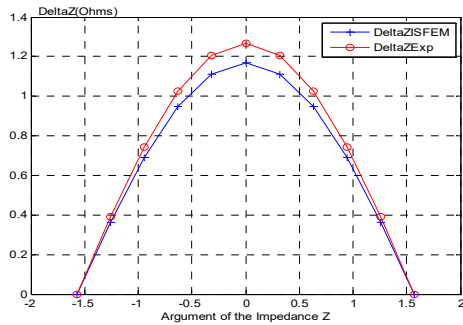


Fig.9. Comparison between stochastic and experimental impedance

In figure 10, we can easily see the presence of the crack for a penetration of 10% and 90%, which correspond respectively to the standard deviation E_c of 0.1 and 0.9

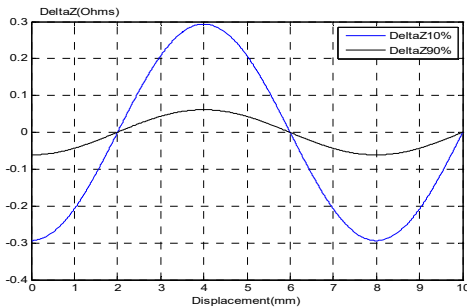


Fig.10. Comparison of impedance variation for different standard deviations

In figure 11, we represented the variation of the real part of the impedance for the two orientations of fibers, longitudinal and transverse, we note that It is noted that the variation of the impedance is more important for $\theta = 0^\circ$ (axis x) compared to the orientation according to the axis y, where $\theta = 90^\circ$.

This comes down to the fact that, the eddy current axis induced is in the direction of the fiber. which suggests that eddy currents are stretched in the direction of high conductivity (Longitudinal) and constricted in the direction of low conductivity (Transverse).

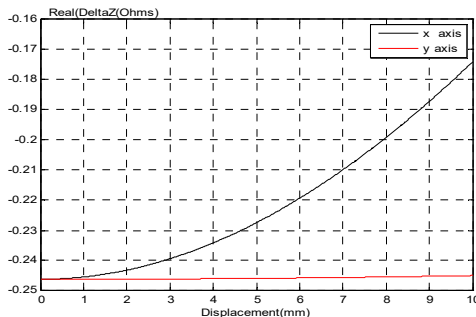


Fig.11. Real part of the variation of the impedances in the directions 0° and 90°

Figure 12 shows the evolution of the reliability index, for two standard deviations 0.5 and 0.9. The theory recommends a reliability index greater than 3 [17]

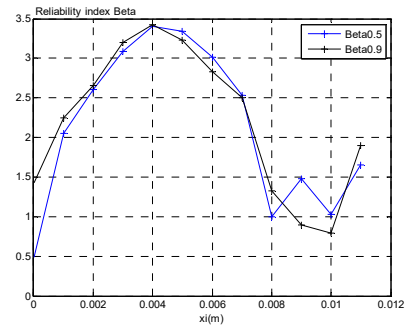


Fig.12. Representation of the Beta reliability index in the crack for different standard deviations

Figure 13 represents the flowchart under Matlab of the different stages of construction of the intrusive stochastic model, its resolution as well as the exploitation of the results

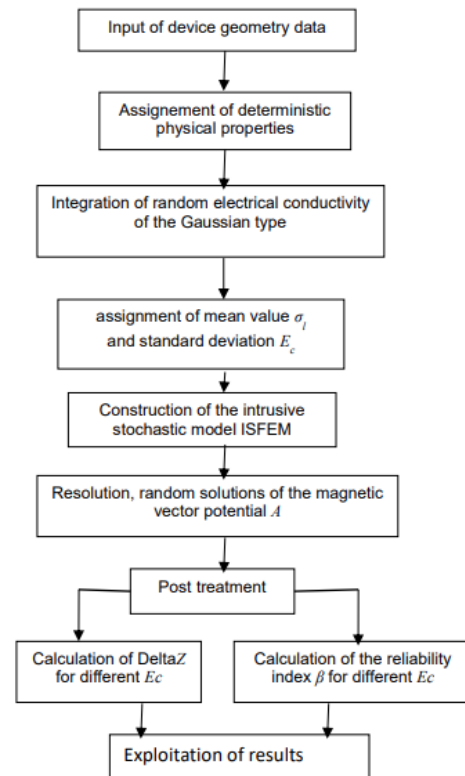


Fig.13. Synthesis flowchart under Matlab

Conclusion

The stochastic finite element method is used to develop an intrusive SFEM model under Matlab environment. The model uses the magnetic vector potential as a state variable and provides the impedance Z of the differential sensor for the reliability analysis of non-destructive testing systems.

The electrical conductivity is considered to be a relevant physical property to characterize the uncertainty of the defect zone of a composite material.

It assumes random values whose standard deviation is taken as the crack penetration rate parameter. Initially, the model is applied to a test specimen in Inconel600 isotropic material, to evaluate the variation of the impedance for three standard deviations respectively 0.1, 0.5 and 0.9, in the zone of default.

The comparison of the results obtained in terms of impedance by the ISFEM model with those of the

experimental tests, shows an excellent concordance in spite of the approximation of the model in axisymmetric 2D.

After this validation, a second application is carried out on a CFRP type composite specimen, for characterization in terms of impedance with and without fault.

The variation of the impedance is compared to the experimental data of the JSAEM#Problem1 benchmark, for a penetration of 100%, following this validation which reinforces the first application; two standard deviations 0.1 and 0.9 were considered to highlight the defect.

The influence of the orientation of the fibers along the x axis ($\theta=0^\circ$) and the y axis ($\theta=90^\circ$) has been studied, the results obtained are very satisfactory.

The last stage of our study consisted reliability evaluation in terms of reliability index for two standard deviations 0.5 and 0.9.

The results obtained on the reliability analysis are in agreement with the expected theoretical results. These conclude with the validation of the Matlab source code developed based on ISFEM.

Moreover, the proposed ISFEM model has the ability to perform the fault characterizations, as well as the reliability analysis, in a single step and no further iteration is needed, unlike non-intrusive stochastic finite element based codes.

Note that for a single position of the sensor the application consumes approximately 50.81s of simulation time for 6010 nodes and 11955 elements with a 3.4 GHz PC and 218 MB of RAM.

Acknowledgments. We would like to present our sincere thanks, to the director as well as the members of the Research center for Real Time NDT, Chosun University, South Korea, for the welcome of our doctoral student and for having made possible the experimental tests on the Inconel600.

Authors: PhD student. *Thinhinane Mahmoudi*, Numerical Modeling of Electromagnetic Phenomena and Components Laboratory, Mouloud Mammeri University of Tizi-Ouzou, BP17 RP 15000, Algeria, E-mail: mahmoudi.thinhinane@gmail.com ; Senior lecturer. *dr. Zehor Oudni*, Electrical engineering department, Mouloud Mammeri University of Tizi-Ouzou, BP 17RP 15000, ALGERIA, E-mail: z_mohellebi@yahoo.fr; *dr. Azouaou Berkache*, IT-based real-time NDT Center, Chosun University, Gwangju, Korea, E-mail: azouaoubk@yahoo.fr; *prof. dr. Jinyi Lee*, Research center for Real Time NDT, Chosun University, 375, Seosuk-dong, Gwangju, 61452, Korea, E-mail: jinyilee@chosun.ac.kr,

The author of correspondence

Senior lecturer. *dr. Zehor Oudni*, Electrical engineering department, Mouloud Mammeri University of Tizi-Ouzou, BP 17RP 15000, ALGERIA, E-mail: z_mohellebi@yahoo.fr;

REFERENCES

- [1] Windels M., Carbon fiber reinforced composites (Sirris), (2013), Retrieved from www.pluscomposites.eu
- [2] Cacciola M., Calcagno S., PIERS, (2006), Online 5, 591.
- [3] Baker A., Composite Materials for Aircraft Structure. Virginia (1986): American Institute of Aeronautics and Astronautics.
- [4] Xiaosong Huang., "Fabrication and Properties of Carbon Fibers," Materials, (2009), Vol. 2, pp. 2369-2403.
- [5] Mook G., Lange R. and Koeser O., Non-destructive characterization of carbon-fibre-reinforced plastics by means of eddy currents, *Composites Science and Technology* 61 (2001), 865–873.
- [6] Prata S. B., and Weldon W. F., "Eddy Current in Anisotropic Composites Applied to Pulsed Machinery", IEEE Trans. Magn., (1996), vol. 32, no. 2, pp. 437-444T.
- [7] Pantelides Chris P., Lawrence D., Clayton R., Burningham A., "Repair of reinforced concrete deep beams using post-tensioned CFRP rods," *Composite Structures*, (2015), Vol.1, pp. 256–265.
- [8] Placko D., Dufour I., "Eddy Current Sensors for Nondestructive Inspection of Graphite Composite Materials", In the IEEE Industry Applications Society Annual Meeting, Texas, USA, (1992), pp.1676 – 1682.
- [9] Khebbab M., Feliachi M., El Hadi Latreche M., Application of finite elements heterogeneous multi-scale method to eddy currents non destructive testing of carbon composites material, *Eur. Phys. J. Appl. Phys.* 80, (2018), 10401.
- [10] Mizutani Y., Todoroki A., Suzuki Y., Mizukami K., "Detection of in-plane and out-of-plane fiber waviness in unidirectional carbon fiber reinforced composites using eddy current testing," *Composites Part B*, (2016), vol. 86, no. 1359-8368, pp. 84-94.
- [11] Oudni Z., Feliachi M., Mohellebi H., Assessment of the Probability of Failure for EC Nondestructive Testing Based on Intrusive Spectral Stochastic Finite Element Method, *Eur. Phys. J. Appl. Phys.* 66 (2014), No.5, 133-137.
- [12] Takagi T., Hashimoto M., Fukutomi H., Miya K., Tsuboi H., Tanaka M., Tani J., Serizawa T., Harada Y., Okano E. and Murakami R., Benchmark models of eddy current testing for steam generator tube: Experiment and numerical analysis, *Intern. J. Applied Electromagn. Mater.* 5 (1994), 149–162.
- [13] Efremov A., Karpenko O., and Udpa L., Generalized multifrequency fusion algorithm for defect detection in eddy current inspection data, *NDT and E International*, (2022) PII: S0963-8695(22)00053-6, JNDT 102654. doi.org/10.1016/j.ndteint.2022.102654,
- [14] Pranesh S., Ghosh D., A FETI-DP based parallel hybrid stochastic finite element method for large stochastic systems, *Computers and Structures*, (2018), Vol. 195, No. CA,
- [15] Lee J., Berkache A., Wang D. and Hwang Y-Ha., Three-Dimensional Imaging of Metallic Grain by Stacking the Microscopic Images, *Appl. Sci.* (2021), 11, 7787. doi.org/10.3390/app11177787
- [16] Berkache A., Lee J., Wang D. and Park D-G., Development of an Eddy Current Test Configuration for Welded Carbon Steel Pipes under the Change in Physical Properties, *Appl. Sci.* (2022), 12, 93. doi.org/10.3390/app12010093
- [17] Loeve M., Probability Theory I, fourth edition, Springer-Verlag Inc, 45 (1977), DOI 10.1007/978-1-4684-9464-8
- [18] Da Silva JRC R. A., Beck A. T., Da Rosa E., Solution of the stochastic beam bending problem by Galerkin Method and the Askey-Wiener scheme, *Latin American Journal of Solids and Structures*, (2009), 6, pp 51 - 72.